Revealing the pseudogap in $Sr_3(Ru_{0.985}Fe_{0.015})_2O_7$ by optical spectroscopy

W. J. Ban,[1] B. Xu,[2] W. H. Li,[3] Y. Wang,[4] J. J. Ge,[4] P. G. Li,[4] R. Yang,[3] Y. M. Dai,[5] Z. Q. Mao,[4] and H. Xiao[1,*]

[1]*Center for High Pressure Science and Technology Advanced Research, Beijing 100094, China*

[2]*University of Fribourg, Department of Physics and Fribourg Center for Nanomaterials, Chemin du Musée 3, CH-1700 Fribourg, Switzerland*

[3]*Institute of Physics, Chinese Academy of Sciences, Beijing 100190, China*

[4]*Department of Physics and Engineering Physics, Tulane University, New Orleans, Louisiana 70118, USA*

[5]*Center for Superconducting Physics and Materials, National Laboratory of Solid State Microstructures and Department of Physics, Nanjing University, Nanjing 210093, China*

(Received 11 April 2018; revised manuscript received 25 July 2018; published 6 November 2018)

We report resistivity, magnetization, and optical spectroscopy study on single-crystal sample of $Sr_3(Ru_{0.985}Fe_{0.015})_2O_7$. An upturn is observed in resistivity at about 30 K. Below 30 K, the dip in resistivity $R(\omega)$, the suppression in scattering rate $1/\tau(\omega)$, the peaklike feature in optical conductivity $\sigma_1(\omega)$, and the remainder of spectral weight all suggest the formation of a pseudogap. In addition, one phonon peak at about 600 cm^{-1} is distinguished at all temperatures, which has asymmetric line shape. Such asymmetric line shape can be fit by a Fano function, and the resulting Fano factor $1/q^2$ and linewidth γ show significant increases below 30 K, giving further evidence for the formation of a pseudogap, which might originate from the partial k-space gap opening due to density wave instability.

DOI: 10.1103/PhysRevB.98.205111

I. INTRODUCTION

The Ruddlesden-Popper-type $(Ba,Sr,Ca)_{n+1}Ru_nO_{3n+1}$ $(n = 0, 1, 2, \ldots, \infty)$ materials have attracted significant attention because of the existence of rich electronic and magnetic phenomena in these materials, such as superconductivity, complex magnetism, metal-insulator transition (MIT), density wave (DW), quantum criticality, and heavy fermions as well as pseudogaps (PG) [1–22]. PG phenomena have been intensively investigated in high-T_C superconductors (HTSC) because of their possible connection to the superconducting mechanisms [23–28]. PG phenomena have also been widely observed and investigated in $(Ba,Sr,Ca)_{n+1}Ru_nO_{3n+1}$ $(n = 0, 1, 2, \ldots, \infty)$ series compounds. For example, the early optical spectroscopy study of Sr_2RuO_4 exhibited a gaplike behavior with a gap energy of 6.3 meV [22]. It could be coupled to gapped magnetic excitations, reminding us of the PG behavior in HTSC. The optical conductivity spectra of four-layer and nine-layer $BaRuO_3$ compounds clearly displayed the formation of a PG [20,21]; however, four-layer $BaRuO_3$ shows a metallic Fermi-liquid-like behavior, while nine-layer $BaRuO_3$ has an insulator-like state at low temperature.

A quite interesting observation is that PG have also been widely observed in some strongly correlated materials near their resistivity-upturn temperature. For example, the optical spectroscopy study of $Ca_3Ru_2O_7$ shows a PG opening around 200 cm^{-1} below 50 K, accompanied with an upturn of the resistivity at 48 K, which might be attributed to the partial gap opening due to the DW instability [29]. For $Sr_3Ru_2O_7$, with Ru site doping by a few percent of Mn, optical spectroscopy study shows the opening of a gap accompanied by the resistivity-upturn behavior [18]; however, because of the lack of data below 600 cm^{-1}, the authors could not address whether there is a Drude-like peak as the compound enters the ground state below its resistivity-upturn temperature, so the optical data are not sufficient to discuss whether there is a full gap or pseudogap opening phenomenon [30].

$Sr_3Ru_2O_7$ is a paramagnetic metal and a system with strong magnetic fluctuations [11,12,31–33]. So, the introduction of a magnetic field and magnetic doping can induce very interesting effects on the magnetic and electronic properties. The magnetic neutron scattering study of $Sr_3Ru_2O_7$ shows that the application of a magnetic field can tune it through two magnetically ordered spin density wave (SDW) states. Manganese-doped $Sr_3Ru_2O_7$ exhibits a commensurate E-type AFM order, accompanied by a resistivity-upturn behavior [18,19,34,35]. However, $Sr_3(Ru_{1-x}Fe_x)_2O_7$ with Fe substitution for Ru shows a metallic spin-glass-like state for $x = 0.01$, whereas an insulating-like, E-type AFM ordered phase is induced below $T_N \approx 40$ K for $x \geqslant 0.03$, respectively [15].

To determine whether the PG opening phenomenon also exists in Fe-doped $Sr_3Ru_2O_7$ and to reveal more information about the resistivity-upturn behavior, we perform resistivity and optical spectroscopy studies on a single-crystal sample of $Sr_3(Ru_{0.985}Fe_{0.015})_2O_7$. The resistivity shows a clear upturn at about 30 K. Below 30 K, a clear dip in resistivity $R(\omega)$ and a peaklike feature in optical conductivity $\sigma_1(\omega)$ were observed in far infrared range, accompanied by the suppression in scattering rate $1/\tau(\omega)$ and the remainder of spectral weight (SW), suggesting the formation of a PG. In addition, a phonon peak at about 600 cm^{-1} has asymmetric line shape, which can be fit by a Fano function, and the resulting Fano factor $1/q^2$ and linewidth γ show significant increases, accompanied by the resistivity-upturn behavior, giving further evidence for the formation of a PG.

*hong.xiao@hpstar.ac.cn

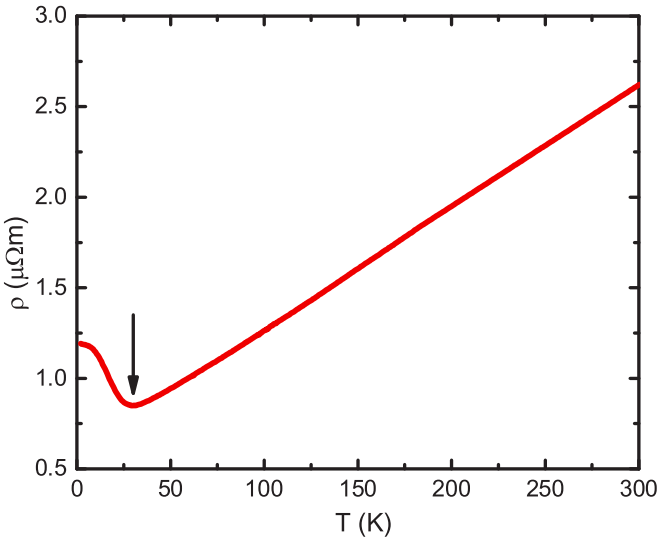

FIG. 1. The temperature-dependent resistivity ρ of $Sr_3(Ru_{0.985}Fe_{0.015})_2O_7$. The black arrow denotes the resistivity-upturn temperature.

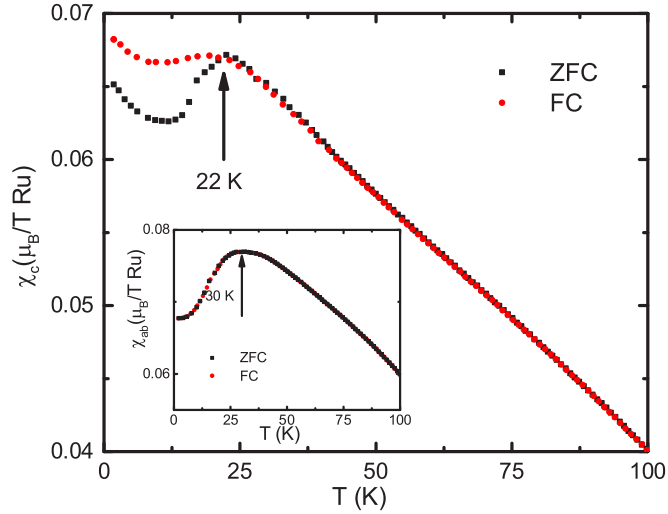

FIG. 2. The temperature-dependent magnetic susceptibility χ_c of $Sr_3(Ru_{0.985}Fe_{0.015})_2O_7$ measured under zero-field-cooled (ZFC) and field-cooled (FC) conditions. Inset: χ_{ab} vs T under ZFC and FC.

II. EXPERIMENTAL DETAILS

High-quality $Sr_3(Ru_{1-x}Fe_x)_2O_7$ single crystals were grown using the floating zone technique [15]. The resulting crystals have dimensions of several millimeters. The actual Fe level was determined to be 0.015 by energy-dispersive x-ray (EDX) measurements on the as-grown single crystals. The dc resistivity was measured by a four-probe method, and the electrical current flows along the direction parallel to the *ab* plane of the crystal. The measurement was conducted on a commercial Quantum Design Physical Properties Measurement System (PPMS). The magnetic susceptibility was measured on a Quantum Design superconducting quantum interference device vibrating sample magnetometer system (SQUID-VSM). The optical reflectance measurements were performed on as-grown shiny surface of a single crystal with a Fourier transform infrared spectrometer (Bruker 80v) in the frequency range from 40 to 20000 cm^{-1}. An *in situ* gold and aluminum overcoating technique was used to get the reflectance [36]. The measured reflectance was then corrected by multiplying the available curves of gold and aluminum reflectivity at different temperatures. The real part of conductivity $\sigma_1(\omega)$ was obtained by the Kramers-Kronig transformation of $R(\omega)$. The Hagen-Rubens relation was used for low-frequency extrapolation; on the high-frequency side, we employed an extrapolation method with x-ray atomic scattering functions [37]. This new extrapolation method is proven to be more effective and unambiguous in deriving and analyzing the optical constants.

III. RESULTS AND DISCUSSIONS

Figure 1 presents the temperature dependence of resistivity for $Sr_3(Ru_{0.985}Fe_{0.015})_2O_7$ single crystal. Upon cooling, the resistivity decreases continuously until 30 K. Below this temperature, the resistivity shows a clear upturn. Similar behaviors have been observed in Fe/Ti/Mn-doped $Sr_3Ru_2O_7$ [15,17,18] and $Ca_3Ru_2O_7$ [29].

Figure 2 shows the temperature dependence of the magnetic susceptibility χ of $Sr_3(Ru_{0.985}Fe_{0.015})_2O_7$ under zero-field-cooled (ZFC) and field-cooled (FC) conditions, respectively. A sharp peak develops in magnetic susceptibility χ_{ab} at about 30 K, suggestive of an onset of paramagnetic-antiferromagnetic phase transition. However, χ_c shows a bifurcation between the ZFC and FC data below about 22 K, characteristic of a spin-glass-like state, similar to $Sr_3(Ru_{0.985}Fe_{0.01})_2O_7$, which shows a paramagnetic-antiferromagnetic phase transition at about 10 K and enters a spin-glass-like state at 4 K [15].

Figure 3(a) shows the reflectance spectra $R(\omega)$ of $Sr_3(Ru_{0.985}Fe_{0.015})_2O_7$ from 0 to 1500 cm^{-1} at several temperatures 35, 50, 100, 200, and 300 K, which are above the resistivity-upturn temperature. The high value of $R(\omega)$ which increases upon cooling reflects the metallic nature of this material.

However, below the resistivity-upturn temperature, the low frequency $R(\omega)$ decreases upon cooling [Fig. 3(b)], consistent with the upturn of the resistivity, and $R(\omega)$ becomes strongly suppressed in the region between 0 to 6500 cm^{-1} [inset of Fig. 3(a)], while a clear diplike feature [as indicated by the black arrow in Fig. 3(b)] gradually developed at about 270 cm^{-1} and the lower ω reflectance increases faster than those of higher temperatures, which is a gaplike feature manifested in reflectance spectra. Besides, one phonon mode at about 600 cm^{-1} emerges in $R(\omega)$ at all temperatures, as indicated by the red arrow.

More insight into the evolution of the electronic states across the resistivity-upturn temperature is clearly reflected in the optical conductivity spectra. Figure 4(a) illustrates the real part of optical conductivity $\sigma_1(\omega)$ at several temperatures below 50 K. The most prominent behavior in $\sigma_1(\omega)$ is that below the resistivity-upturn temperature, the SW below about 200 cm^{-1} becomes gradually suppressed, and the suppressed SW partially transfer to a peaklike feature with its central frequency at about 350 cm^{-1} [shown as the blue circle in Fig. 4(a)], which is a gaplike feature manifested in

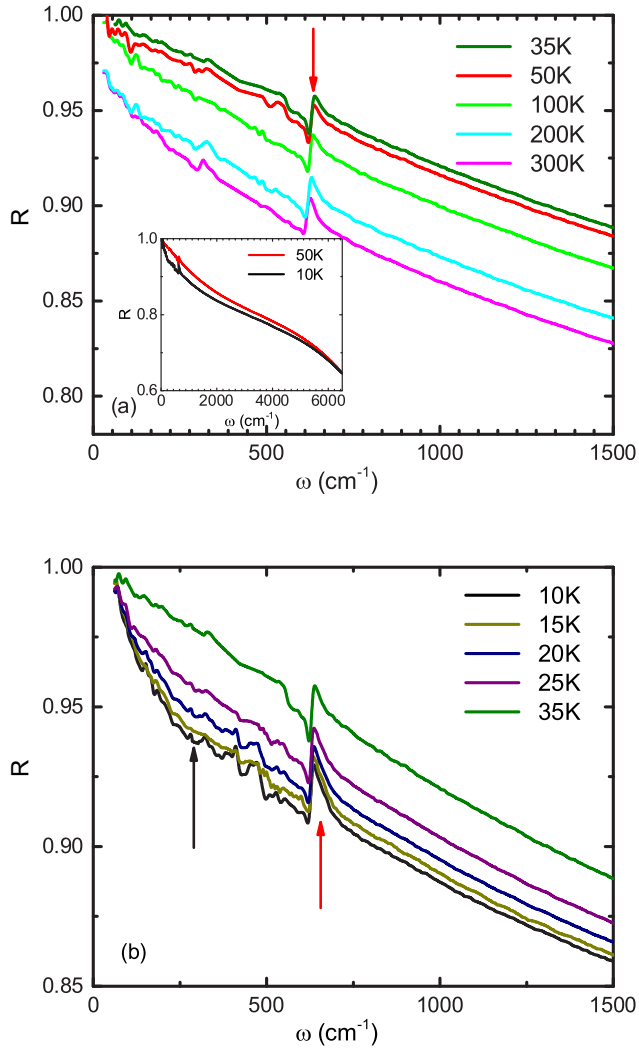

FIG. 3. (a) The reflectance spectra $R(\omega)$ of $Sr_3(Ru_{0.985}Fe_{0.015})_2O_7$ from 0 to 1500 cm^{-1} at several temperatures above 35 K. (b) The reflectance spectra $R(\omega)$ of $Sr_3(Ru_{0.985}Fe_{0.015})_2O_7$ from 0 to 1500 cm^{-1} at several temperatures below 35 K. The inset in panel (a) show the reflectivity of 10 and 50 K up to 6500 cm^{-1}. The black arrow denotes the diplike feature in reflectance spectra. The red arrows denote the phonons.

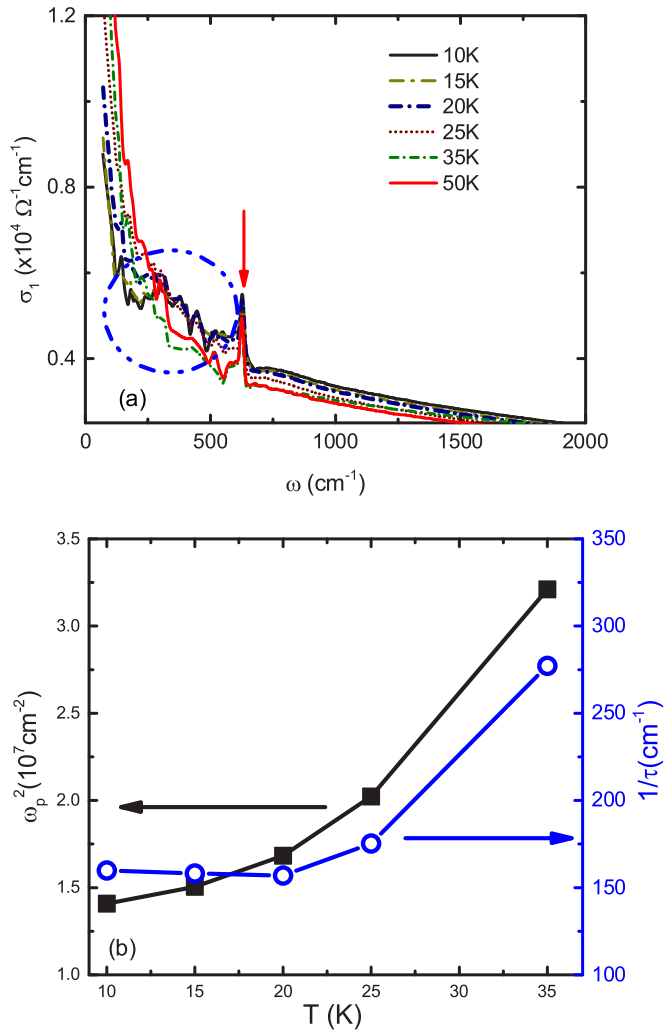

FIG. 4. (a) The temperature-dependent optical conductivity $\sigma_1(\omega)$ of $Sr_3(Ru_{0.985}Fe_{0.015})_2O_7$ at several temperatures below 50 K. The blue circle indicates the energy region of the peaklike feature which appears below 35 K. The red arrow denotes the phonons. (b) The temperature dependence of the plasma frequency ω_p^2 and scattering rate $1/\tau$.

conductivity spectra [29]. It is interesting to note that as frequency decreases below about 180 cm^{-1}, $\sigma_1(\omega)$ increases and a very narrow Drude-type component appears; this feature is different from the formation of an ordinary band gap insulating (or a semiconducting) state, where the SW in the gaplike region should disappear completely. The remainder of the SW below the resistivity-upturn temperature indicates that a PG is formed in this material.

To investigate the SW transfer more clearly, we have calculated the integrated SW between different lower and upper cutoff frequencies, which was defined as $W_S = \int_a^b \sigma_1(\omega)d\omega$. Figure 5(a) illustrates the upper cutoff frequency-dependent SW at several representative temperatures. The ratio of W_S at low to high temperature $W_S(T_L)/W_S(T_H)$ is shown in Fig. 5(b). W_S(50 K)/W_S(300 K) exceeds 1 at low energy and then smoothly approaches 1, which indicates a transfer of SW from high- to low-energy region with decreasing temperature. The W_S transfer across the resistivity-upturn temperature can be more clearly seen in the plot of the ratio of the integrated SW at two different temperatures below and above 30 K, e.g., W_S(10 K) / W_S(50 K). The ratio is less than 1 at lower energy due to the opening of a PG in the $\sigma_1(\omega)$ spectrum at 10 K. Eventually, the SW is nearly recovered and the ratio approaches 1 at much higher energies. We also calculate the W_S in three different energy intervals: 40–280, 280–20000, and 40–20 000 cm^{-1}. The temperature dependences of the normalized SW, $W_S(T)/W_S$(300 K), are displayed in Figs. 5(c), 5(d), and 5(e). It can be found that the overall spectral weight between 40 and 20 000 cm^{-1} is temperature independent, and above 30 K, the SW transfers from the 280–20000 to 40–280 cm^{-1} regions upon cooling, which is induced by the Drude components narrowing. Below the resistivity-upturn temperature, the SW transfers from the

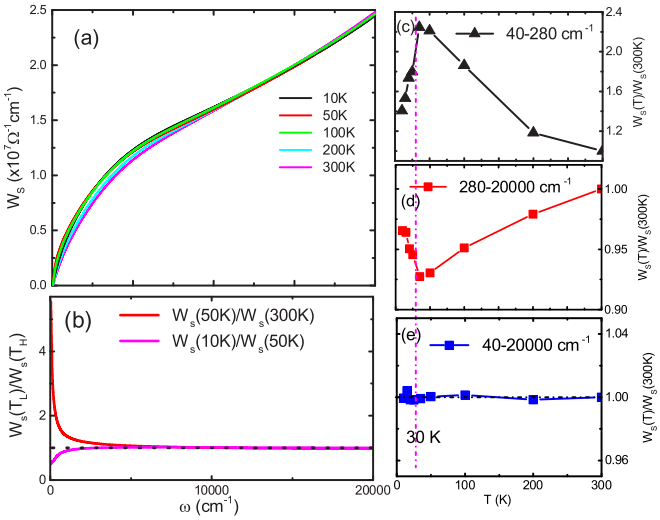

FIG. 5. (a) Upper cutoff frequency-dependent SW at several representative temperatures of $Sr_3(Ru_{0.985}Fe_{0.015})_2O_7$. (b) The frequency dependence of $W_S(T_L)/W_S(T_H)$. [(c), (d), (e)] The temperature dependence of $W_S(T)/W_S(300\ \mathrm{K})$ between different lower and upper cutoff frequencies.

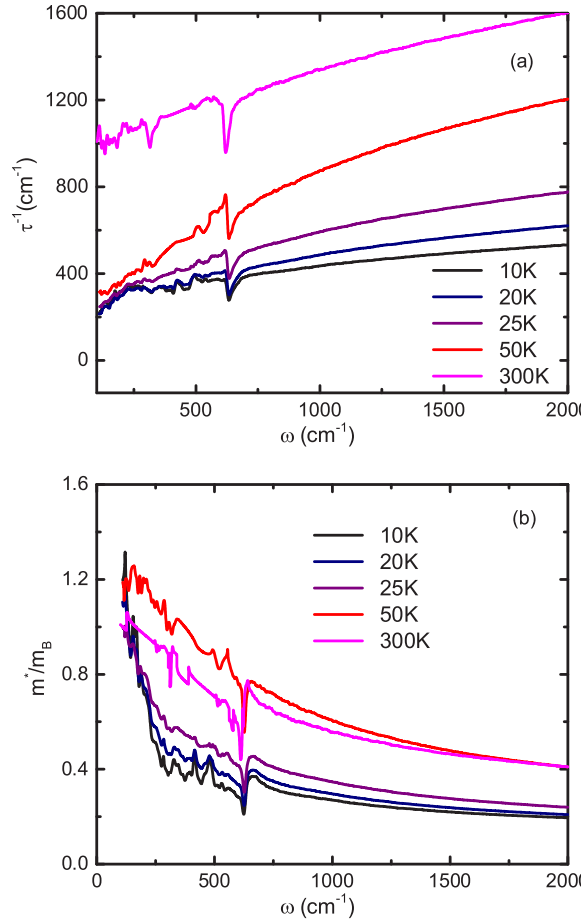

FIG. 6. Temperature-dependent (a) scattering rate $1/\tau(\omega)$ and (b) effective mass m^*/m_B derived from the extended Drude model analysis.

40–280 to 280–20 000 cm^{-1} regions, further confirming the formation of a PG.

In order to elucidate the change in electrodynamics responding to the PG opening, we analyze the coherent peak quantitatively. First of all, the plasma frequency ω_p is estimated by calculating the low-ω SW, $\omega_p^2 = 8\int_0^{\omega_c}\sigma_1(\omega)d\omega$. The cutoff frequency ω_c is chosen so as to make the integration cover all contributions from free carriers and exclude contributions from interband transitions. Usually, the integral goes to a frequency where $\sigma_1(\omega)$ shows a minimum value. We expect there is a balance between the Drude component tail and the onset part of interband transition. So we choose $\omega_c = 220\ \mathrm{cm}^{-1}$. As the PG develops, ω_p^2 decreases as temperature decreases, as shown in Fig. 4(b). Second, we estimate scattering rate $1/\tau$ using the relation $1/\tau = (1/4\pi)\rho\omega_p^2$. As the PG develops, $1/\tau$ [shown in Fig. 4(b)] also decreases as temperature decreases. The upturn of $\rho(T)$ below 30 K (shown in Fig. 1) could be due to the fact that ω_p^2 decreases more rapidly than $1/\tau$. Similar phenomena have been observed in $Ca_3Ru_2O_7$ and 4H and 9R $BaRuO_3$ compounds, which also possess the PG formation [20,21].

We also analyze the optical conductivity with the extended Drude model; in this approach, the simple Drude model is extended by making the damping term in the Drude formula complex and frequency dependent [38–40]. Here the scattering rate and the effective mass are allowed to have frequency dependence:

$$\frac{1}{\tau(\omega)} = \frac{\omega_p^2}{4\pi}\frac{\sigma_1(\omega)}{\sigma_1^2(\omega)+\sigma_2^2(\omega)}, \tag{1}$$

$$\frac{m^*}{m_B} = \frac{\omega_p^2}{4\pi\omega}\frac{\sigma_2(\omega)}{\sigma_1^2(\omega)+\sigma_2^2(\omega)}, \tag{2}$$

where m_B is the band mass and ω_p is the plasma frequency estimated by calculating the low-ω SW at corresponding temperatures as mentioned above, shown as Fig. 4(b). The obtained spectra of the scattering rate and the effective mass are displayed in Fig. 6. For clarity, only several representative temperatures are shown: room temperature and just above and below resistivity-upturn temperature.

Both the scattering rate and the effective mass show a pronounced temperature dependence at low frequencies. Notably, the scattering rate is suppressed below about 300 cm^{-1}, and correspondingly, the effective mass is strongly enhanced. Those spectral features can also be taken as the optical signature of the PG state, like the cases in cuprates [38–40], and some DW materials, 2H-TaS_2, Na_xTaS_2 [41], and 2H-$NbSe_2$ [42].

Besides, one phonon peak at about 600 cm^{-1} is distinguished in $\sigma_1(\omega)$ at all temperatures, as shown in Fig. 7(a), which cannot be fit well by the Lorentz model, because of its asymmetric line shape. We extract the phonon line shape by subtracting a linear electronic background in a narrow frequency range at all measured temperatures. It is instructive to fit the phonon line shape with the Fano model [43–48]:

$$\sigma_1(\omega) = \frac{2\pi}{Z_0}\frac{\Omega^2}{\gamma}\frac{q^2+\frac{4q(\omega-\omega_0)}{\gamma}-1}{q^2\left(1+\frac{4(\omega-\omega_0)^2}{\gamma^2}\right)}, \tag{3}$$

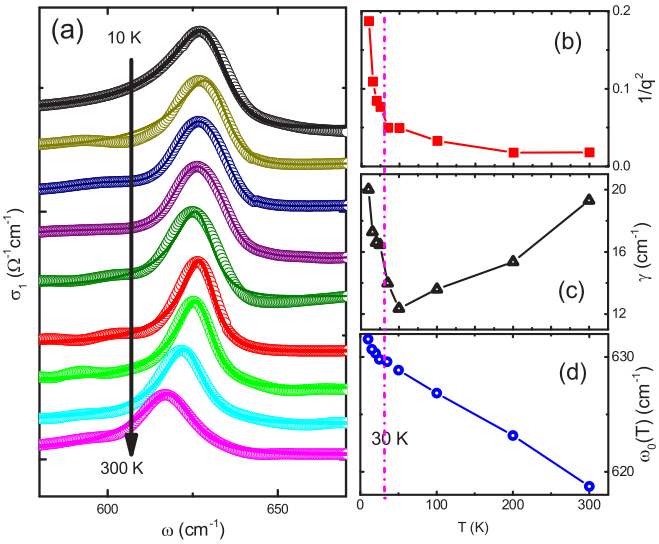

FIG. 7. (a) Line shape of the infrared phonon modes in $Sr_3(Ru_{0.985}Fe_{0.015})_2O_7$. The solid lines through the data denote the Fano fitting results. Temperature dependence of (b) the Fano factor $1/q^2$, (c) the linewidth γ, and (d) the frequency of the phonons. The solid lines are guides to the eye.

where Z_0 is the vacuum impedance and ω_0, γ, and Ω correspond to the phonon frequency, linewidth, and strength of the phonon, respectively. The asymmetric phonon line shape is known to be related to electron-phonon coupling [44–46,49,50] and is typically characterized through the Fano-Breit-Wigner (FBW) parameter q. The physical meaning of q is that it is inversely related to the strength of the electron-phonon coupling. Therefore, a larger $1/q^2$ (the Fano factor) indicates more conspicuous asymmetry in the phonon line shape, while for $1/q^2 = 0$, the symmetric Lorentz line shape is fully recovered. The Fano factors $1/q^2$, determined from the fittings, are shown in Fig. 7(b). We found that above 30 K, $1/q^2$ increases slightly with temperature decreasing; however, below 30 K, it increases significantly, reflecting enhancement of the electron-phonon coupling.

The linewidth γ of the Fano resonance [shown as the black line in Fig. 7(c)] decreases continuously until 30 K, below which temperature, γ shows a clear upturn. For the electron-phonon interaction process, the phonon linewidth γ is indicative of the related electron-phonon coupling strength. However, the phonon linewidth is related to two processes: $\gamma(T) = \gamma^{ph-ph}(T) + \gamma^{e-ph}(T)$, where $\gamma^{e-ph}(T)$ and $\gamma^{ph-ph}(T)$ represent the electron-phonon (e-ph) and anharmonic phonon-phonon (ph-ph) interactions. The e-ph (ph-ph) interaction gives an increasing (decreasing) linewidth as the temperature is reduced. Thus, the temperature dependence of the total γ is a balance of $\gamma^{e\text{-ph}}(T)$ and $\gamma^{ph\text{-ph}}(T)$ [51]. At temperature above 30 K, the electron-phonon coupling is weak; in this case, phonon decay is dominated by the anharmonic effect: A zone-center phonon decays into two acoustic modes with the same frequencies and opposite momenta [52,53], so $\gamma^{\text{ph-ph}}(T)$ dominates. The temperature dependence of the phonon linewidth $\gamma^{\text{ph-ph}}(T)$ for this process follows $\gamma^{\text{ph-ph}}(T) = \gamma_0^{\text{ph-ph}}(1 + \frac{2}{e^{\frac{\hbar\omega_0}{2k_BT}} - 1})$, where $\gamma_0^{\text{ph-ph}}$ is the residual linewidth at zero temperature. Apparently, this model can account for the decreasing γ as the temperature is decreased. At temperature below 30 K, the upturn of γ might be arise from strong electron-phonon coupling mechanism. If the electron-phonon coupling is strong, a phonon can also decay by creating an electron-hole pair [54], resulting in a temperature-dependent phonon linewidth $\gamma^{e\text{-ph}}(T)$, $\gamma^{e\text{-ph}}(T) = \gamma_0^{e\text{-ph}} D_{e-h}(\omega_0, T)$, where $D_{e-h}(\omega_0, T)$ is the finite-temperature joint electron-hole pair density of states at $\hbar\omega_0$ (the energy of the phonon peak).

As mentioned above, we propose that a PG opens below the resistivity-upturn temperature. This results in a suppressed SW at lower frequency transfers to a peaklike feature with its central frequency at about 350 cm^{-1} [shown as the blue circle in Fig. 3(a)]. Thus, this brings up the possibility of changes to the electronic states in this system. That is, the electronic density of states (DOS) increases obviously at the peaklike feature energy region, which could contribute to the increasing γ below 30 K, and results in a significant increase of the electron-phonon coupling. Thus, the line shape of the phonon peaks becomes more asymmetric, leading to a significant increase of $1/q^2$. Therefore, the significant increase of $1/q^2$ and γ in the present study can be attributed to the formation of the peaklike structure around 350 cm^{-1}. Thus, the temperature evolution of $1/q^2$ and γ gives further evidence for the opening of a PG accompanied by the resistivity-upturn behavior. Similar enhancement of Fano factor was also reported in $CaFeO_3$ [50] and was attributed to the changing of the electron-phonon coupling and the electronic DOS due to a gap opening feature below a charge-disproportionation transition temperature. In addition, we show the temperature dependence of the phonon frequency (ω_0) in Fig. 7(d). It corresponds to the peak frequency of the in-plane Ru-O stretching mode [55,56] and exhibits the usual hardening for decreasing temperature, due to the crystal contraction.

It is remarkable that $Sr_3(Ru_{0.985}Fe_{0.015})_2O_7$ shows PG phenomena coherently in transport and optical properties. To understand the origin of the PG in $Sr_3(Ru_{0.985}Fe_{0.015})_2O_7$, there are several experimental facts which should be taken into account. First of all, the dip in $R(\omega)$ and corresponding peaklike feature in $\sigma_1(\omega)$ may remind us of DW materials. As for a DW order, the opening of an energy gap leads to a SW suppression below 2Δ (the energy gap) and a non-symmetric peak with clear edgelike feature near 2Δ in the optical conductivity. Second, the observed PG features are similar to four-layer, nine-layer $BaRuO_3$ compounds [20,21] and isostructural compound $Ca_3Ru_2O_7$ [29], where the PG were ascribed to the partial gap opening due to the DW instability. Third, for $Sr_3Ru_2O_7$, due to its strong magnetic fluctuations, a magnetic field and magnetic impurities can profoundly affect the magnetic and electronic properties. The magnetic neutron scattering study of $Sr_3Ru_2O_7$ shows that the application of a magnetic field can tune it through two magnetically ordered spin density wave (SDW) states [57]. Hence, the doping of magnetic impurities (Fe) may act as the role of a magnetic field with the possibility to induce SDW order. Further study is required regarding the formation of a DW order in $Sr_3(Ru_{0.985}Fe_{0.015})_2O_7$. Nevertheless, the dip in $R(\omega)$ and corresponding peaklike feature in $\sigma_1(\omega)$, accompanied by the enhancement of $1/q^2$ and γ below the resistivity-upturn

temperature, are sufficient enough to indicate that there is a PG opening behavior.

IV. CONCLUSION

In summary, an upturn of the resistivity is observed in $Sr_3(Ru_{0.985}Fe_{0.015})_2O_7$ at about 30 K. Optical spectroscopy studies find a clear dip in $R(\omega)$, which corresponds to a peaklike feature in $\sigma_1(\omega)$ and a suppression in scattering rate $1/\tau(\omega)$, indicating the formation of a PG accompanied with the resistivity-upturn behavior. Moreover, the significant increase of Fano factor $1/q^2$ and linewidth γ below this temperature gives further evidence for the opening of a PG, which might originate from the partial k-space gap opening due to DW instability.

ACKNOWLEDGMENTS

We would like to thank N. L. Wang and Z. G. Chen for the experimental facility and assistance for optical reflectance measurements, and acknowledge the support of NSAF, Grant No. U1530402. The work (single crystal growth and characterization) at Tulane is supported by the U.S. Department of Energy (DOE) under EPSCoR Grant No. DE-SC0012432 with additional support from the Louisiana Board of Regents.

[1] Y. Yoshida, I. Nagai, S.-I. Ikeda, N. Shirakawa, M. Kosaka, and N. Môri, Phys. Rev. B **69**, 220411 (2004).
[2] N. Kikugawa, A. W. Rost, C. W. Hicks, A. J. Schofield, and A. P. Mackenzie, J. Phys. Soc. Jpn. **79**, 024704 (2010).
[3] A. P. Mackenzie and Y. Maeno, Rev. Mod. Phys. **75**, 657 (2003).
[4] Y. Maeno, S. Kittaka, T. Nomura, S. Yonezawa, and K. Ishida, J. Phys. Soc. Jpn. **81**, 011009 (2012).
[5] S. Nakatsuji and Y. Maeno, Phys. Rev. Lett. **84**, 2666 (2000).
[6] G. Cao, S. McCall, J. E. Crow, and R. P. Guertin, Phys. Rev. Lett. **78**, 1751 (1997).
[7] W. Bao, Z. Q. Mao, Z. Qu, and J. W. Lynn, Phys. Rev. Lett. **100**, 247203 (2008).
[8] S.-I. Ikeda, Y. Maeno, S. Nakatsuji, M. Kosaka, and Y. Uwatoko, Phys. Rev. B **62**, R6089 (2000).
[9] S. A. Grigera, R. S. Perry, A. J. Schofield, M. Chiao, S. R. Julian, G. G. Lonzarich, S. I. Ikeda, Y. Maeno, A. J. Millis, and A. P. Mackenzie, Science **294**, 329 (2001).
[10] R. A. Borzi, S. A. Grigera, J. Farrell, R. S. Perry, S. J. S. Lister, S. L. Lee, D. A. Tennant, Y. Maeno, and A. P. Mackenzie, Science **315**, 214 (2007).
[11] L. Capogna, E. M. Forgan, S. M. Hayden, A. Wildes, J. A. Duffy, A. P. Mackenzie, R. S. Perry, S. Ikeda, Y. Maeno, and S. P. Brown, Phys. Rev. B **67**, 012504 (2003).
[12] K. Kitagawa, K. Ishida, R. S. Perry, T. Tayama, T. Sakakibara, and Y. Maeno, Phys. Rev. Lett. **95**, 127001 (2005).
[13] E. Dagotto, Science **309**, 257 (2005).
[14] Z. Fang and K. Terakura, Phys. Rev. B **64**, 020509 (2001).
[15] M. Zhu, Y. Wang, P. G. Li, J. J. Ge, W. Tian, D. Keavney, Z. Q. Mao, and X. Ke, Phys. Rev. B **95**, 174430 (2017).
[16] C. Mirri, F. M. Vitucci, P. Di Pietro, S. Lupi, R. Fittipaldi, V. Granata, A. Vecchione, U. Schade, and P. Calvani, Phys. Rev. B **85**, 235124 (2012).
[17] P. Steffens, J. Farrell, S. Price, A. P. Mackenzie, Y. Sidis, K. Schmalzl, and M. Braden, Phys. Rev. B **79**, 054422 (2009).
[18] R. Mathieu, A. Asamitsu, Y. Kaneko, J. P. He, X. Z. Yu, R. Kumai, Y. Onose, N. Takeshita, T. Arima, H. Takagi, and Y. Tokura, Phys. Rev. B **72**, 092404 (2005).
[19] M. A. Hossain, B. Bohnenbuck, Y. D. Chuang, M. W. Haverkort, I. S. Elfimov, A. Tanaka, A. G. Cruz Gonzalez, Z. Hu, H.-J. Lin, C. T. Chen, R. Mathieu, Y. Tokura, Y. Yoshida, L. H. Tjeng, Z. Hussain, B. Keimer, G. A. Sawatzky, and A. Damascelli, Phys. Rev. B **86**, 041102 (2012).
[20] Y. S. Lee, J. S. Lee, K. W. Kim, T. W. Noh, J. Yu, Y. Bang, M. K. Lee, and C. B. Eom, Phys. Rev. B **64**, 165109 (2001).
[21] Y. S. Lee, J. S. Lee, K. W. Kim, T. W. Noh, J. Yu, E. J. Choi, G. Cao, and J. E. Crow, Europhys. Lett. **55**, 280 (2001).
[22] K. Pucher, A. Loidl, N. Kikugawa, and Y. Maeno, Phys. Rev. B **68**, 214502 (2003).
[23] H. Ding, T. Yokoya, J. C. Campuzano, T. Takahashi, M. Randeria, M. R. Norman, T. Mochiku, K. Kadowaki, and J. Giapintzakis, Nature (London) **382**, 51 (1996).
[24] M. R. Norman, H. Ding, M. Randeria, J. C. Campuzano, T. Yokoya, T. Takeuchi, T. Takahashi, T. Mochiku, K. Kadowaki, P. Guptasarma, and D. G. Hinks, Nature (London) **392**, 157 (1998).
[25] C. Renner, B. Revaz, J.-Y. Genoud, K. Kadowaki, and O. Fischer, Phys. Rev. Lett. **80**, 149 (1998).
[26] Y. M. Dai, B. Xu, P. Cheng, H. Q. Luo, H. H. Wen, X. G. Qiu, and R. P. S. M. Lobo, Phys. Rev. B **85**, 092504 (2012).
[27] T. Dong, F. Zhou, and N. L. Wang, Phys. Rev. B **88**, 184507 (2013).
[28] S. J. Moon, Y. S. Lee, A. A. Schafgans, A. V. Chubukov, S. Kasahara, T. Shibauchi, T. Terashima, Y. Matsuda, M. A. Tanatar, R. Prozorov, A. Thaler, P. C. Canfield, S. L. Bud'ko, A. S. Sefat, D. Mandrus, K. Segawa, Y. Ando, and D. N. Basov, Phys. Rev. B **90**, 014503 (2014).
[29] J. S. Lee, S. J. Moon, B. J. Yang, J. Yu, U. Schade, Y. Yoshida, S.-I. Ikeda, and T. W. Noh, Phys. Rev. Lett. **98**, 097403 (2007).
[30] M. Imada, A. Fujimori, and Y. Tokura, Rev. Mod. Phys. **70**, 1039 (1998).
[31] D. J. Singh and I. I. Mazin, Phys. Rev. B **63**, 165101 (2001).
[32] M. B. Stone, M. D. Lumsden, R. Jin, B. C. Sales, D. Mandrus, S. E. Nagler, and Y. Qiu, Phys. Rev. B **73**, 174426 (2006).
[33] S. Ramos, E. Forgan, C. Bowell, S. Hayden, A. Schofield, A. Wildes, E. Yelland, S. Brown, M. Laver, R. Perry, and Y. Maeno, Physica B **403**, 1270 (2008).
[34] D. Mesa, F. Ye, S. Chi, J. A. Fernandez-Baca, W. Tian, B. Hu, R. Jin, E. W. Plummer, and J. Zhang, Phys. Rev. B **85**, 180410 (2012).
[35] B. Hu, G. T. McCandless, V. O. Garlea, S. Stadler, Y. Xiong, J. Y. Chan, E. W. Plummer, and R. Jin, Phys. Rev. B **84**, 174411 (2011).
[36] C. C. Homes, M. Reedyk, D. A. Cradles, and T. Timusk, Appl. Opt. **32**, 2976 (1993).
[37] D. B. Tanner, Phys. Rev. B **91**, 035123 (2015).
[38] D. N. Basov and T. Timusk, Rev. Mod. Phys. **77**, 721 (2005).
[39] P. B. Allen, Phys. Rev. B **3**, 305 (1971).

[40] A. V. Puchkov, D. N. Basov, and T. Timusk, J. Phys.: Condens. Matter **8**, 10049 (1996).
[41] W. Z. Hu, G. Li, J. Yan, H. H. Wen, G. Wu, X. H. Chen, and N. L. Wang, Phys. Rev. B **76**, 045103 (2007).
[42] S. V. Dordevic, D. N. Basov, R. C. Dynes, and E. Bucher, Phys. Rev. B **64**, 161103 (2001).
[43] R. Yang, Y. Dai, B. Xu, W. Zhang, Z. Qiu, Q. Sui, C. C. Homes, and X. Qiu, Phys. Rev. B **95**, 064506 (2017).
[44] B. Xu, Y. Dai, J. Han, K. Wang, R. Yang, Y. Yang, W. Zhang, H. Xiao, and X. Qiu, Physica C (Amsterdam, Neth.) **503**, 25 (2014).
[45] W. J. Padilla, M. Dumm, S. Komiya, Y. Ando, and D. N. Basov, Phys. Rev. B **72**, 205101 (2005).
[46] A. B. Kuzmenko, L. Benfatto, E. Cappelluti, I. Crassee, D. van der Marel, P. Blake, K. S. Novoselov, and A. K. Geim, Phys. Rev. Lett. **103**, 116804 (2009).
[47] B. Xu, Y. M. Dai, B. Shen, H. Xiao, Z. R. Ye, A. Forget, D. Colson, D. L. Feng, H. H. Wen, C. C. Homes, X. G. Qiu, and R. P. S. M. Lobo, Phys. Rev. B **91**, 104510 (2015).
[48] B. Xu, H. Xiao, B. Gao, Y. H. Ma, G. Mu, P. Marsik, E. Sheveleva, F. Lyzwa, Y. M. Dai, R. P. S. M. Lobo, and C. Bernhard, Phys. Rev. B **97**, 195110 (2018).
[49] K.-Y. Choi, Y. G. Pashkevich, K. V. Lamonova, H. Kageyama, Y. Ueda, and P. Lemmens, Phys. Rev. B **68**, 104418 (2003).
[50] C. X. Zhang, H. L. Xia, H. Liu, Y. M. Dai, B. Xu, R. Yang, Z. Y. Qiu, Q. T. Sui, Y. W. Long, S. Meng, and X. G. Qiu, Phys. Rev. B **95**, 064104 (2017).
[51] B. Xu, Y. Dai, L. Zhao, K. Wang, R. Yang, W. Zhang, J. Liu, H. Xiao, G. Chen, S. Trugman, J.-X. Zhu, A. Taylor, D. Yarotski, R. Prasankumar, and X. Qiu, Nat. Commun. **8**, 14933 (2017).
[52] P. G. Klemens, Phys. Rev. **148**, 845 (1966).
[53] J. Menéndez and M. Cardona, Phys. Rev. B **29**, 2051 (1984).
[54] N. Bonini, M. Lazzeri, N. Marzari, and F. Mauri, Phys. Rev. Lett. **99**, 176802 (2007).
[55] C. Mirri, L. Baldassarre, S. Lupi, M. Ortolani, R. Fittipaldi, A. Vecchione, and P. Calvani, Phys. Rev. B **78**, 155132 (2008).
[56] J. S. Lee, Y. S. Lee, T. W. Noh, S. Nakatsuji, H. Fukazawa, R. S. Perry, Y. Maeno, Y. Yoshida, S. I. Ikeda, J. Yu, and C. B. Eom, Phys. Rev. B **70**, 085103 (2004).
[57] C. Lester, S. Ramos, R. S. Perry, T. P. Croft, R. I. Bewley, T. Guidi, P. Manuel, D. D. Khalyavin, E. M. Forgan, and S. M. Hayden, Nat. Mater. **14**, 373 (2015).